

DBCD-MIT: A Dynamic Model for Breast Cancer Detection using Multi-Input Thermograms

Mahsa Ensafi¹, Mohammad Reza Keyvanpour^{1*}, Seyed Vahab Shojaedini²

¹Department of Computer Engineering, Faculty of Engineering and Technology, Alzahra University, Tehran, Iran

²Biomedical Engineering Department, Iranian Research Organization for Science and Technology (IROST), Tehran, Iran

Abstract

Introduction: Breast cancer mortality rates could be significantly reduced through early detection. In the past decade, thermal imaging has been introduced to detect this type of cancer. Although non-invasive, painless, and low-cost, the images generated by this method require machine learning methods for analysis.

Methods: It is common for artificial intelligence systems to analyze thermograms based on a single input of thermography images or to feed thermograms from different views to a single input detection model without any processing to extract dependencies and eliminate redundancies. Using multi-input thermography images in different views correlated with practical correlated information, this article presents a method for detecting breast cancer. To estimate dependencies between thermograms in parallel with removing redundancy, dynamically and separately made filters are used for different views.

Results: Finally, fusing the information based on their effectiveness in improving the performance of the deep neural network may increase the accuracy of the proposed method in diagnosing the occurrence of breast cancer. In comparison with existing methods, the proposed mechanism can significantly increase breast cancer diagnosis. Experimental results showed that the proposed procedure improved sensitivity and specificity by 1-14 percent and 1-25 percent, respectively, compared to deep learning or handcrafted approaches.

Conclusion: Because thermographic images are usually taken from multiple views and the fact that dynamic filters enhance the information extracted from different views, the module presented in this article is an appropriate component for thermogram-based breast cancer classifiers.

Keywords: Thermography, Breast cancer, Deep learning, Diverse perspectives, Adaptive filtering

Article History:

Received: 3 October 2024

Accepted: 27 December 2024

Please cite this paper as:

Ensafi M, Keyvanpour MR, Shojaedini SV. DBCD-MIT: A Dynamic Model for Breast Cancer Detection using Multi-Input Thermograms. Health Man & Info Sci. 2025; 12(1): 41-56. doi: 10.30476/jhmi.2025.105355.1260.

*Correspondence to:

Mohammad Reza Keyvanpour,
Department of Computer
Engineering, Faculty of
Engineering, Alzahra University,
Tehran, Iran

Email: keyvanpour@alzahra.ac.ir

Introduction

Cancer is one of the deadliest diseases in the world, according to the World Health Organization (WHO) (1). A cancerous tumor is a growth of abnormal cells that can be benign or malignant (2). Cancer types differ in their location and degree of severity. More than 100 types of cancer are named based on the organ or tissue (3).

Breast cancer is one of the most common types of cancer. The use of different imaging techniques makes detection easier and reduces mortality rates for this type of cancer (4). Several different screening procedures are used to detect breast cancer, including mammography, histopathology, ultrasound imaging, and thermography.

The most common method of screening for breast cancer is mammography (5). However, this method has several disadvantages, including the requirement of expensive equipment (6) and its low accuracy for women with dense breasts. Radiation used during mammography also increases the risk of breast cancer, as some patients complain of anxiety and pain caused by compression of the breast area (7, 8). Histopathology is a standard screening method in which a pathologist examines a tissue sample by taking microscopic images in the laboratory. This method may be limited in its utility because of its invasive nature and dependence upon physician expertise. Furthermore, this method is expensive and time-consuming (9). Ultrasound imaging is another screening modality for

breast cancer, which penetrates the breast with sound waves that are safer than X-rays (9). This method's low image contrast and low sensitivity make it complementary to mammography (7). Due to its non-invasive, painless, and low-cost nature, thermography has gained popularity among researchers in recent years (10). This method detects breast lesions by measuring skin temperature distribution (10). Cancer cells have a higher metabolic rate than healthy tissues, which results in higher temperatures (6). Thermograms are created by converting heat emitted from the breast into visual information (5). Any woman of any age can use thermal imaging for breast cancer screening, even if their breasts are dense (11).

The manual processing of thermograms requires expertise from physicians and is time-consuming and tedious. Also, poor quality and noise may reduce diagnostic accuracy and increase unnecessary biopsies (12). Recent developments in computer processing capacity, machine learning algorithms, and GPU-based cloud computing resources have contributed to the success of computer-aided diagnosis systems in interpreting breast thermographic images (8). The majority of published articles on thermographic imaging for breast cancer diagnosis use traditional machine learning. These methods involve manually extracting features such as pixel value, texture, orientation, and shape by a data expert. These systems perform well, providing features that can be accurately identified or extracted (13). Recently, deep learning has received much attention in the field of computer-aided disease diagnosis (14). A deep learning algorithm can automatically extract features from input data (5).

The article (15) investigates image normalization and automatic Classification. After normalization, features from thermogram images were extracted, including statistical measures and texture characteristics. Machine learning classifiers, such as Support Vector Machines (SVMs) and Artificial Neural Networks (ANNs), were trained for automatic Classification. The article (9) proposes a hybrid method combining dynamic and static infrared thermography for abnormal screening and breast cancer diagnosis. By clustering time series data, the authors screened the breast, identifying malignant tumors through texture feature extraction; however, this method

has a high execution time. In the article (16), Zernike and Haralick's features are extracted based on the geometry and texture of cancerous breast tissue. The authors evaluated various classifiers, including ANN and decision trees, for classifying cysts and benign and malignant lesions; however, this resulted in low sensitivity values for breast cancer detection. The study in (17) analyzed bilateral symmetry between the left and right breasts by comparing thermal patterns and hot spot characteristics, extracting texture features via Gray-Level Co-occurrence Matrices (GLCMs) to train a machine learning classifier (e.g., SVM) for detecting abnormalities. Similarly, researchers (18) introduced a dual thresholding approach, extracting features like area, perimeter, and temperature differences to classify thermograms as normal or abnormal using SVM. In (19), diverse feature extraction techniques, including texture, thermal asymmetry, and shape features, were evaluated with classifiers like SVM, Random Forests (RF), and Neural Networks. Traditional methods rely on manual feature extraction, which is challenging, while deep learning, particularly Convolutional Neural Networks (CNNs), automates feature learning and has gained prominence in medical imaging (20, 21).

The study (22) compared two machine learning techniques - CNNs and SVMs - for detecting breast cancer using thermograms. The CNN-based approach used a CNN to extract relevant features from the thermograms automatically. The SVM-based approach involved manually engineering features like geometrical and textural, which were then used to train an SVM classifier to categorize the thermograms. The article (3) reports the development of a software system that can automatically analyze thermograms to detect breast cancer. In the article (23), the performance of CNN in detecting breast cancer in thermograms is compared to some other classification techniques, including Tree Random Forest (TRF), Multi-Layer Perceptron (MLP), and Bayes Network (BN). As a result of this study, CNN provided more accurate results than the other alternative algorithms. However, based on (24), this method is sensitive to noisy and irrelevant features. In (25), the thermograms are classified using CNN after applying preprocessing and segmentation techniques. The key innovation in the (26) approach is the use of

deep learning techniques, specifically CNNs, for both the segmentation of breast regions and the Classification of abnormalities.

CNNs require extensive training data due to their high number of parameters, but public and labeled datasets for medical applications, especially breast cancer detection via thermograms, are limited. Transfer learning with pre-trained models addresses this challenge (27). Studies highlight using models such as ResNet34, ResNet50, DenseNet121, MobileNetV2, and VGG16.

ResNet34 and ResNet50 achieved the best performance in (26), while DenseNet121 (28) utilized edge detection (Prewitt and Roberts) for feature extraction in a three-channel architecture. MobileNetV2 (29) was fine-tuned with thermal images for Classification. The article (30) utilized the pre-trained VGG16 model as the backbone of their breast cancer diagnosis system. To enhance the feature extraction capabilities of the VGG16 model, the researchers incorporated deep attention mechanisms into the network. Researchers (31) expanded the CNN model with deep attention mechanisms to enhance the network's ability to extract features. The authors of (32) proposed a novel breast cancer screening system based on a Capsule Network (Caps Net) architecture. The Caps Net model was designed to take the multi-view (front, left, and right) breast thermal infrared images as input. The model fused the information from the different views to make a more informed breast cancer screening decision.

Thermograms for breast cancer detection can be obtained from five views: frontal and two laterals on each side. Most studies focus on frontal views, often overlooking the additional information multiple perspectives provide. Few

studies have examined the interdependencies between features across different views. A dynamic model, DBCD-MIT, is proposed to address this gap for enhanced breast cancer detection using multi-input thermograms.

DBCD-MIT: The Proposed Method

The diagnosis in single-input systems is based only on one of the sets of thermograms obtained from the patient. Therefore, thermograms taken from other patient views are not considered when making the final decision. The neglected thermograms may contain valuable information that may otherwise be overlooked in the single-input system. Consequently, the performance of the single-input system depends on the single-input thermogram, which is often compromised by various factors, such as poor data quality. It is possible to consider a system that increases the reliability of the final decision by combining the features of all multi-inputs received from the patient and deciding based on the resulting combination. According to this approach, the decision is made based on all the patient's thermograms. Due to the greater number of inputs in the multi-input system, this system is more noise-resistant.

Furthermore, in the single-input system, a A patient's thermogram can be identified from one view of a healthy person and another view of a sick person. This problem is not present with the multi-input system; therefore, the rate of false positives and negatives is reduced, and reliability is improved. The main structure of the proposed DBCD-MIT is shown in Figure 1. Table 1 defines some of the notations used to describe the proposed system. According to Figure 1, the inputs of DBCD-MIT

Table 1: Notations and variables used in the proposed method

Symbol	Description
DBCD-MIT	Dynamic model for Breast Cancer Detection using Multi-Input Thermograms
FF	Feature vector of the Frontal view
FLL	Feature vector of the Lateral Left 45 ° view
FSL	The Feature vector of the Side-view Left 90 ° view
FLR	Feature vector of the Lateral Right 45 ° view
FSR	The Feature vector of the Side-view Right 90 ° view
FE	Feature Extractor
FW	Feature Weighting
WFF	Weighted Feature vector of the Frontal view
WFLL	Weighted Feature vector of the Lateral Left 45 ° view
WFSL	The Weighted Feature vector of the Side-view Left 90 ° view
WFLR	Weighted Feature vector of the Lateral Right 45 ° view
WFSR	Weighted Feature vector of the Side-view Right 90 ° view
TWF	Total of Weighted Features

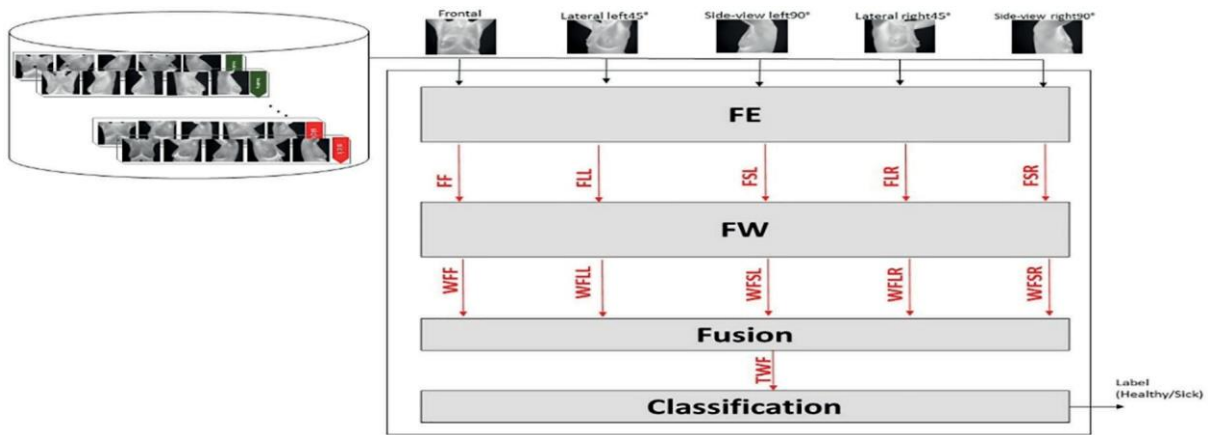


Figure 1: General structure of the DBCD-MIT method

consist of patients’ thermograms in five views, such as frontal, lateral left 45 °, side-view left 90 °, lateral right 45 °, and side-view right 90 °, and output is a patient’s label (healthy or sick). As specified in Figure 1, DBCD-MIT involves four basic components: Feature Extractor (FE) block, Feature Weighting (FW) block, Fusion, and Classification.

During the first step, the features of each patient’s thermograms are extracted separately. Then, in this system, each thermogram is weighed according to its usefulness. This feature set is then fused in the next step. Upon fusion of the features, a single feature is obtained, and classification is made according to it, and the patient’s thermograms are predicted at the end. Below are the details of the methods used in each component described in Figure 1.

Feature Extractor

The features of each thermogram are extracted in this part of the proposed DBCD-MIT system. An illustration of the internal structure of the Feature Extractor (FE) block can be found in Figure 2. As can be seen from Figure 2, this block’s inputs and outputs are the patient’s thermograms and feature vectors in

different views, respectively. First, the necessary preprocessing is applied to extract the feature. An automatic feature extraction process is then carried out using CNNs.

Preprocessing

An important step in the automatic processing of medical images is the preprocessing of the input data. This step aims to improve the image quality, decrease noise, and remove unwanted portions of the image. As a result of the preprocessing of data, the results of subsequent processes are improved (13). This study used some preprocessing techniques in order to achieve this goal. The first step is to remove blurred and bandaged thermograms. Blurred thermograms may not provide fine and original details. A few thermograms were also bandaged due to surgical reasons. This cover may damage the thermal pattern of the breast. Feature extraction occurs following the Output of the Preprocessing (OP) stage, as shown in Figure 2.

CNN

This stage is represented learning, which facilitates extracting features from various views. Since the patient’s thermograms from different

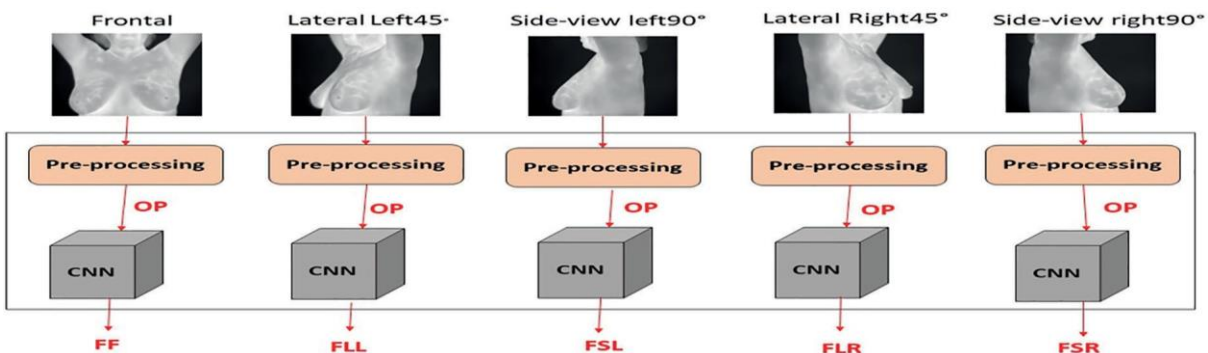


Figure 2: The internal structure of the FE block

Table 2: Details of the utilized deep models

Network	Structure	Parameters
VGG16	13 convolution 5 max pooling	138,357,544
VGG19	16 convolution 5 max pooling	143,667,240
InceptionV3	48 layers deep	23,851,784
Xception	71 layers deep	22,910,480
ResNet50	50 layers deep	25,636,712
DenseNet121	121 layers deep	8,062,504

views contain additional information, and learning the features of this system will produce more comprehensive data from the patient than the single-input system. Figure 2 illustrates how a convolutional neural network extracts the features of each thermogram in the corresponding view. To extract features, transfer learning is used. The transfer learning concept is further applied as an efficient method since CNN requires extensive data for automatic feature extraction (5). VGG16, VGG19, InceptionV3, Xception, ResNet50, and DenseNet121 are the networks used in this experiment. The internal structure of the tested networks is shown in Table 2.

Feature Weighting

Figure 1 illustrates that the Feature Weighting (FW) block's inputs is the FE block's outputs. The purpose of the FW block is to identify features that have a greater potential for discrimination. Thus, the output of this block is a dynamically weighted vector of input features. An illustration of the internal structure the FW block is found in Figure 3. According to Figure 3, the FW block is

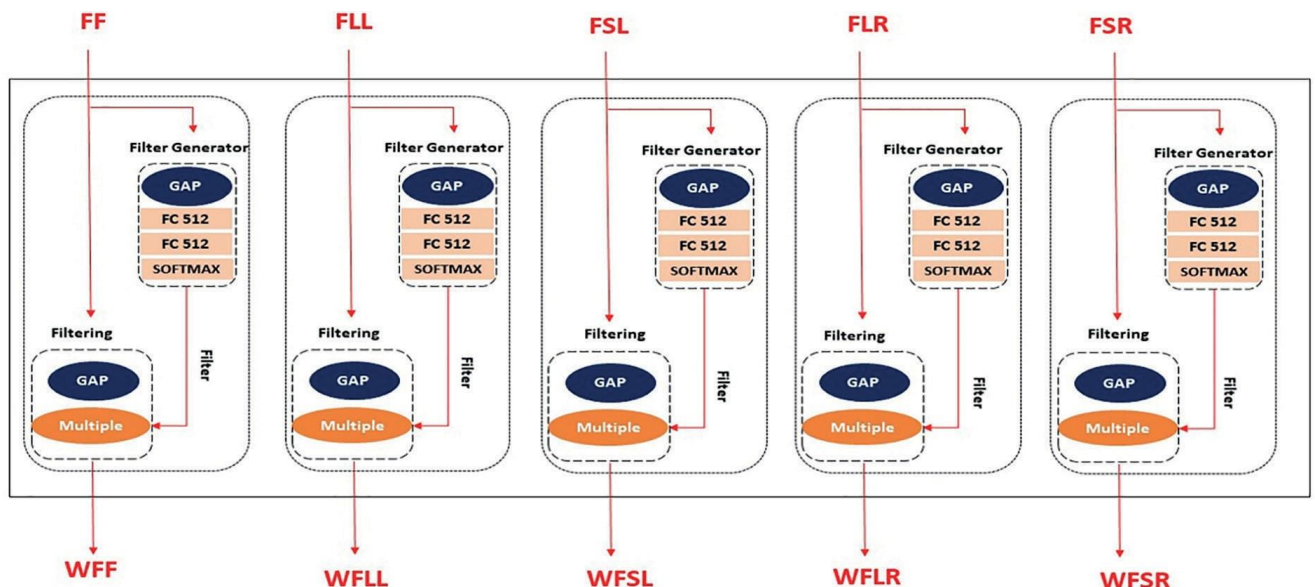
divided into several sub-blocks. The sub-blocks in different views correspond to the feature vectors.

Human vision consists of selectively focusing on a part of information at just the right time and place while ignoring other visually apparent information. The filters in a traditional convolutional neural network are stable after training. However, this study introduces a new framework where filters can be dynamically generated for each view of the thermogram input. The sub-block objective is to identify helpful features of the relevant thermogram and to design new filters based on those features.

After this step, the primary features are filtered according to the produced filters. Feature maps are read from the input in different views and then sent to the next stage as filtered feature vectors. Figure 3 illustrates each sub-block containing two sections called Filter Generator and Filtering.

Filter Generator

According to the input, a special filter is produced in the Filter Generator (FG) block. The

**Figure 3:** The internal structure of the FW block

The relationship between the input features may be analyzed using this block, which examines how the features of different views can be used to diagnose whether a patient is healthy or sick. The block consists of the Global Average Pooling (GAP) layer, two fully connected layers, and a SoftMax function. Below is an explanation of how the filter is dynamically generated based on the features of each thermogram view. Initially, the GAP layer converts feature maps into feature vectors. Afterward, these features are fed into the first dense layer. Assuming that FC_i^1 is the feature vector obtained by applying the GAP layer for the i^{th} input, we can display the output of the first dense layer as equation 1.

$$FC_i^1 = \{fc_{1i}^1 \cdot fc_{2i}^1 \dots fc_{512i}^1\} \tag{1}$$

The output of the j^{th} neuron of the first fully connected layer in the j^{th} FG block may be calculated as equation 2:

$$fc_{ji}^1 = \sum_{r=1}^N O_r \times W_{jr} + \beta \tag{2}$$

The values and indicate the size of the output of the GAP layer and the bias of FC_i^1 , respectively. Similarly, the neurons' weights in the second fully connected layer (FC_i^2) are determined. A SoftMax function was also used to determine the importance value of each feature. During this stage, points are assigned to each feature to determine their relative importance. Therefore, the output of the j^{th} FG block output can be shown as equation 3.

$$O_i^j = SOFTMAX(FC_i^2)SOFTMAX(FC_i^2) \tag{3}$$

Filtering

This section will dynamically apply the filter generated from the previous block to the features. Thus, important and practical features are identified. Figure 3 shows two inputs: the filter generated by the FG block and the feature maps obtained from the previous step. Additionally, GAP is used to generate feature vectors from feature maps. A layer containing the multiplication operator is used to apply the generated filter in the primary feature vector. Thus, the output of this block will be a weighted vector of features. Consequently, the output of the filtering sub-block may be viewed as equation 4, in which WFV_i represents the i^{th} Weighted Filtered feature Vector. In addition, FM_i shows the matrix of primary features.

$$WFV_i = filter_i * GAP(FM_i) \tag{4}$$

Fusion

This block combines features from different views into a single one. The purpose of this section is to display the data comprehensively by using the additional information from several views. The output of the fusion block may be calculated as in equation 5. Here, WFV_i represents the weighted feature vector of the i^{th} view. This can be illustrated as follows by concatenating the features in the different views: $all - WFVS = h(WFV1, \dots WFV_i, \dots WFV5)$ (5)

It is important to note that $h(\cdot)$ represents the function in the above relation. A concatenation function is used in this study to fuse The WFM's.

Classification

A significant purpose of this section is to determine the label that will be assigned to the patient. To perform binary Classification, this system utilizes three fully connected layers. To prevent overfitting, dropout layers are used next to fully connected layers. Figure 4 illustrates the internal structure of the classification system proposed for this study.

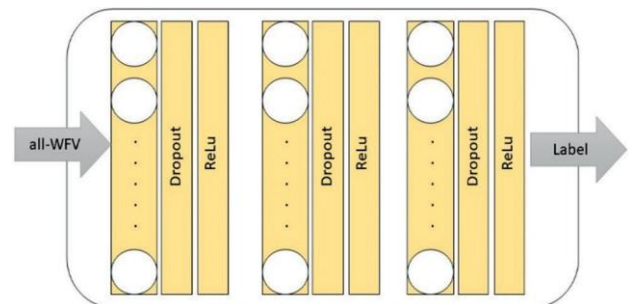


Figure 4: The internal structure of the Classification

Experiment

Dataset

The proposed algorithm was evaluated using a set of breast thermal images, referred to as DMR (33). DMR is a publicly available web platform that provides breast images for the detection of early stages of breast cancer (34). This collection includes thermal images and clinical data in which thermograms with a resolution of 640 x 480 pixels are categorized into healthy and sick. The thermograms were obtained using a static and dynamic protocol. The imaging consisted of a frontal, two laterals of the left at 45° and 90°, and two side-views of the right at 45° and 90° as shown in Figure 5.

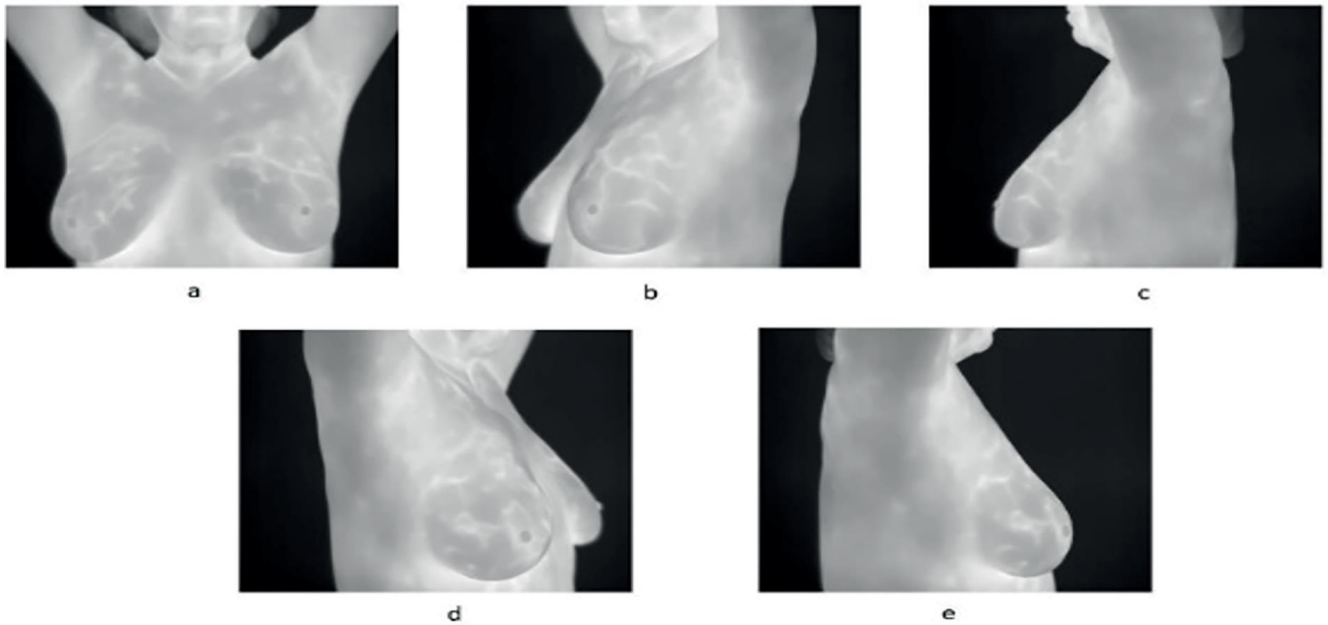


Figure 5: (a) Frontal (b) Lateral left45°(c) Side-view left90° (d) Lateral right45° (e) Side-view right90°

Experimental setup

In experiments of this research, 410 thermograms have been utilized; 205 of them belonged to healthy breasts, and the remaining 205 thermograms belonged to sick breasts. The dataset contains 82 patients, each with five different views of their thermograms, as demonstrated in Table 3.

A fourfold cross-validation strategy was utilized by splitting the dataset into four equal subsets. The learning models were implemented using TensorFlow, an open-source Python library for machine learning. Google Colab, a GPU framework provided by Google, was used to run the program. Table 4 illustrates details of the hyperparameters of the used models.

Evaluation Measures

Following the performance of a test, the obtained results may be interpreted in the following situations. The first case is about

thermograms correctly identified as sick by the model, which are called true positives (TPs). In addition, some cases were misdiagnosed as sick by the classifier, which is called false positives (FPs). In contrast, some cases were classified correctly as healthy by the classifier, which is referred to as true negatives (TN); finally, some cases were misdiagnosed by classifiers as healthy, which are referred to as false negatives (FN). The evaluation criteria used in the state-of-the-art works were also applied in this study to analyze the effectiveness of the proposed method (35).

Accuracy (ACC): Based on equation 6, the accuracy parameter indicates how many samples were correctly identified (healthy and sick).

$$ACC = \frac{TP+TN}{(TP+FP+TN+FN)} \quad (6)$$

Precision (Pre): The precision of the model can be determined by the number of positive cases correctly predicted by the model using equation 7.

$$Pre = \frac{TP}{(TP+FP)} \quad (7)$$

Table 3: Number of used thermograms

	Frontal	Left 45°	Left 90°	Right45°	Right 90°
Healthy	41	41	41	41	41
Sick	41	41	41	41	41
Total	82	82	82	82	82

Table 4: Detailed of hyperparameters

Optimizer	Batch size	Activation function at intermediate layers	Loss function
Adam	16	ReLU	Binary Crossentropy

Sensitivity (Sn): Using equation 8, this parameter indicates how many positive samples were correctly identified.

$$Sn = \frac{TP}{(TP+FN)} \tag{8}$$

Specificity (Sp): Based on equation 9, this parameter represents the number of correctly identified negative samples.

$$Sp = \frac{TN}{(TN+FP)} \tag{9}$$

F-score: The F-score is a measure of precision and sensitivity that considers the impact of adding more penalties, as shown in equation 10 (36).

$$F - score = \frac{2 \times precision \times sensitivity}{precision + sensitivity} \tag{10}$$

Results

Two tests have been designed and run to evaluate the proposed method. According to the authors' previous study on breast cancer diagnosis using thermography, test 1 is designed to investigate the effect of dynamic extraction of the relationship between features in different views. Test 2 examines the proposed method based on deep models and different learning criteria mentioned in the previous section. The difference between the results of these two tests may be considered exactly in the sense of

evaluating the performance of the proposed innovation of this article, which is the use of dynamic filtering in extracting the dependencies between different views and training the neural network with the help of these enriched data. In addition to these two tests, the proposed method has been compared with other methods for a more comprehensive evaluation and comparison. Finally, the proposed method is discussed.

Test 1: The Effect of Dynamic Extraction of the Relationship between Features in Different Views

The authors' previous research (8) tested the idea of including five different views of thermograms without extracting their relationship. For this purpose, three networks, VGG16, InceptionV3, and DenseNet121, were trained and tested with the five views of the thermograms in raw form. Thus, the method mentioned is a basis for comparison with the proposed method in this article. Figure 6 shows the results of the first scenario, which is called the basic single input model, in the rest of the article. Figure 6-a shows thermograms of healthy patients incorrectly classified as sick by the model. Similarly, Figure 6-b illustrates the thermograms of sick patients incorrectly identified as healthy.

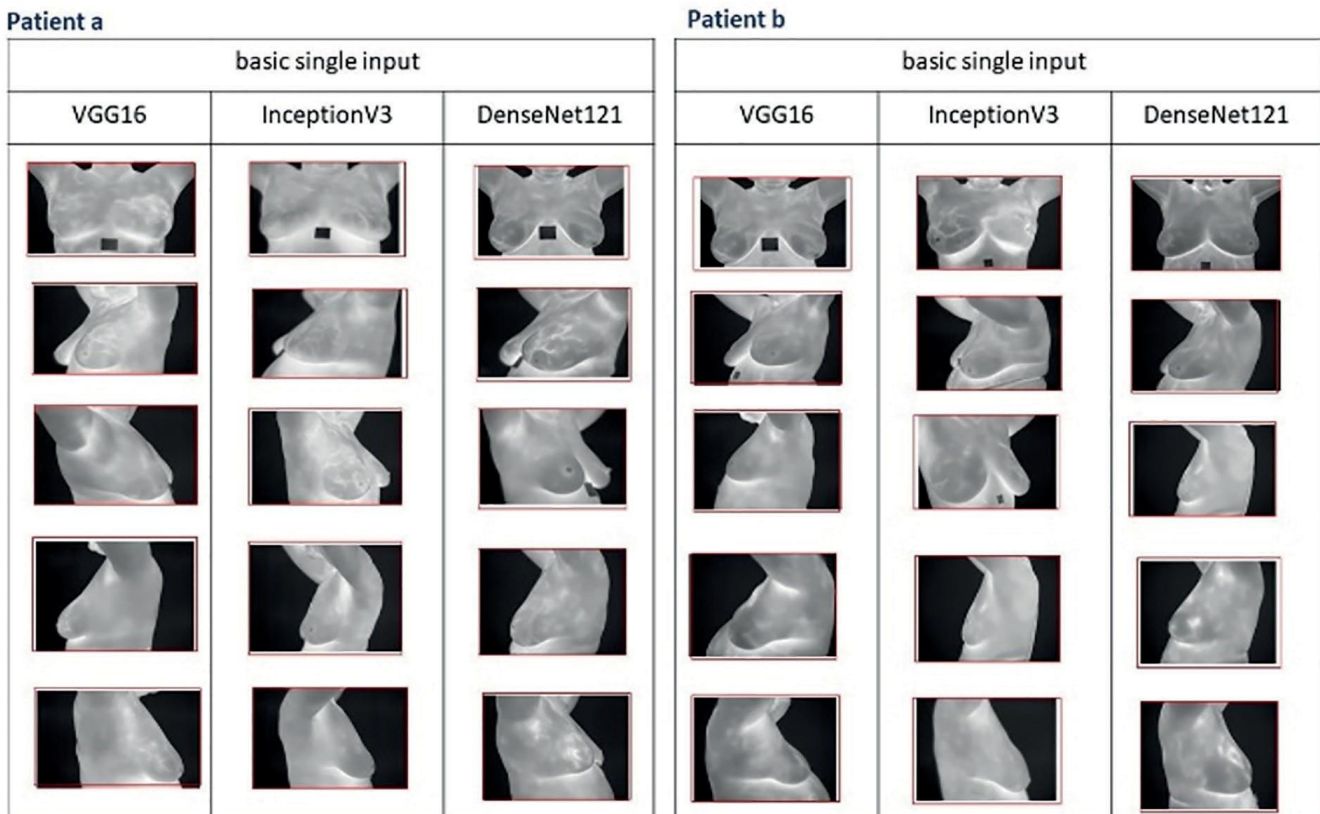


Figure 6: Examples of results of basic single input model: (a) false positive (b) false negative

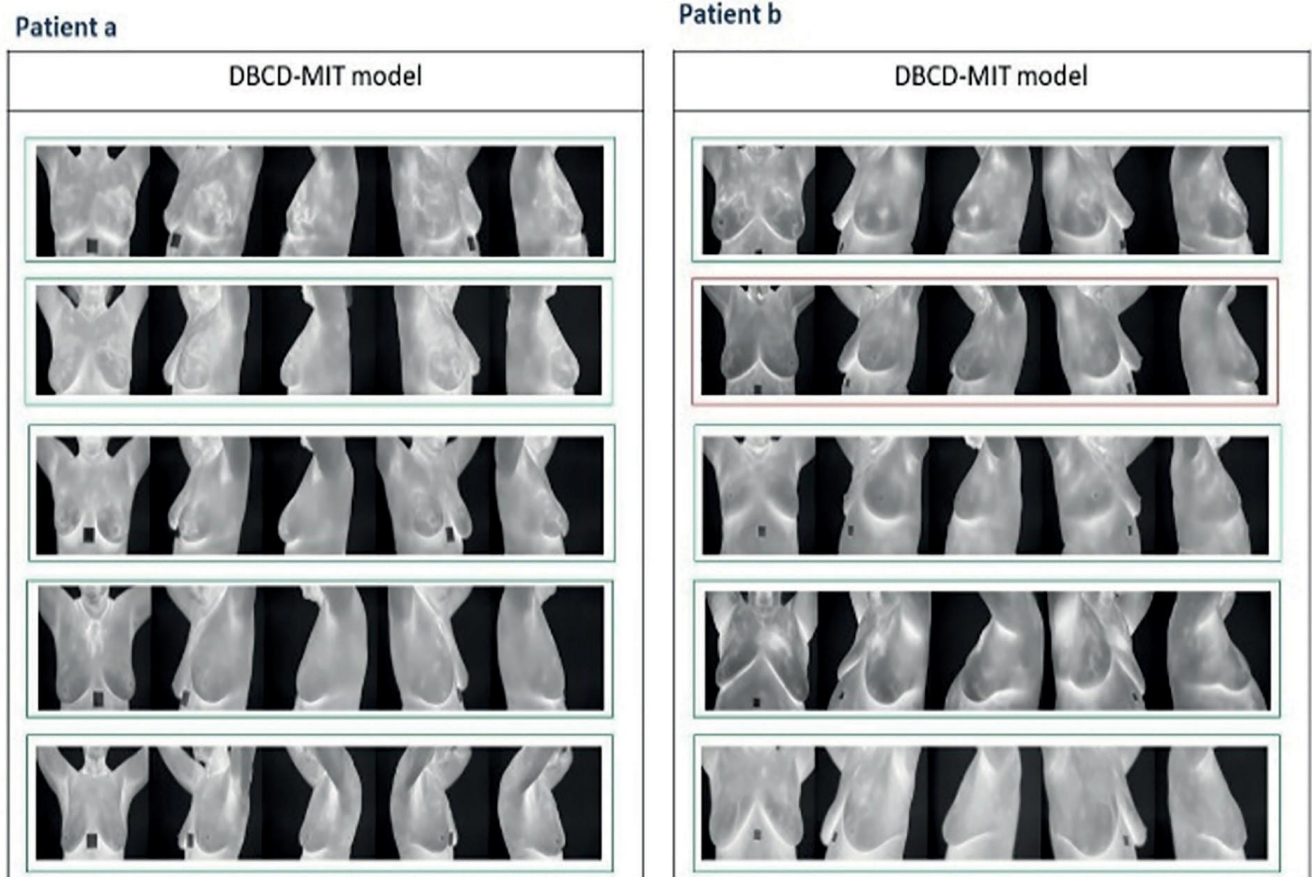


Figure 7: Examples of results of the proposed DBCD-MIT model: (a) true negative, (b) true positive

In contrast, Figure 7 demonstrates the results of the proposed method, which is called the DBCD-MIT model, in the rest of the article. Figure 7-a illustrates the prediction results of the proposed DBCD-MIT model for healthy people after they had been predicted sick previously. Similarly, Figure 7-b shows prediction results from the proposed DBCD-MIT model for sick patients previously predicted from the basic single input model as healthy.

Comparing Figure 6 and Figure 7 demonstrates that by applying the proposed method, many healthy individuals have been

correctly diagnosed as healthy. Furthermore, the majority of sick people are also identified as sick. Meanwhile, one of the sick patients has been mistakenly identified as healthy. According to these results, the proposed method detects healthy and sick patients more accurately than the basic single-input model.

Different labels may be predicted for different patient views in the basic single input model. Based on five thermograms provided by two healthy patients, Figure 8 illustrates the prediction results of both the basic single input model and the proposed DBCD-MIT model.

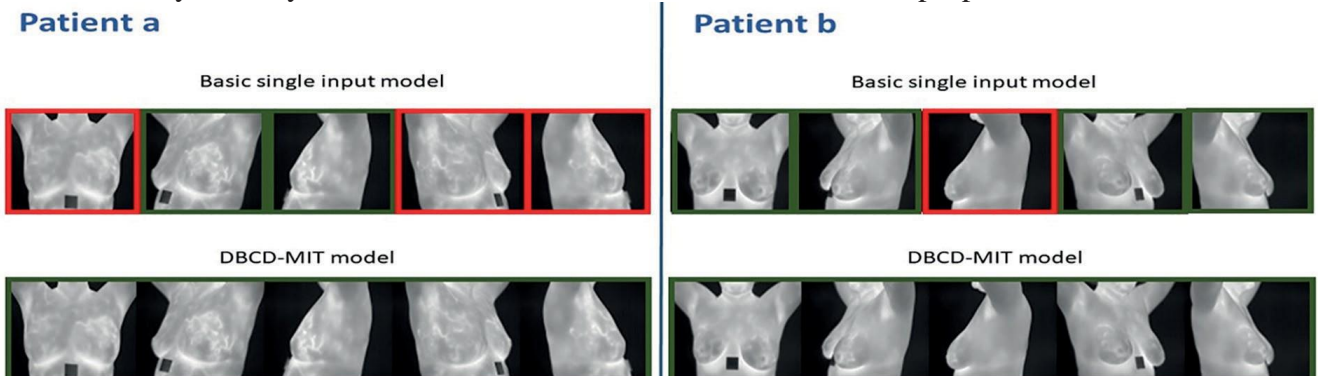


Figure 8: Prediction of two healthy patients

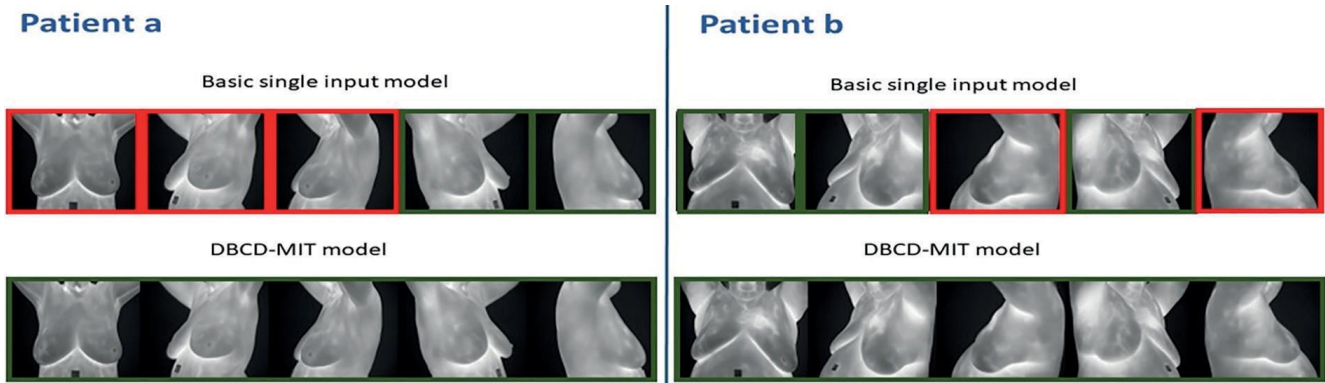


Figure 9: Prediction of two sick patients

As evident from the figure, three thermograms of the patient in the frontal, the lateral right 45 °, and the side-view right 90 ° views were incorrectly classified as sick in the basic scheme. As another example, the side-view left 90 ° view of patient b is incorrectly identified as sick using the basic single input model. These two patients are correctly diagnosed as healthy under the proposed DBCD-MIT model, which means that all five thermograms in five views are predicted to be healthy.

On the other hand, Figure 9 shows the prediction results of both the basic single input model and the proposed DBCD-MIT model when applied to five thermograms provided by two sick patients. It can be seen from the figure that in the basic single input model, three views of patient a, including the frontal, lateral left 45 °, and side-view left 90 °, were incorrectly classified as healthy. As a result of the basic single input model, the side-view left 90 ° and side-view right 90 ° views of the patient b were incorrectly predicted to be healthy. The proposed DBCD-MIT model correctly diagnoses these two patients as sick, i.e., all five thermograms in five views are reported to be sick.

Test 2: The Effect of Different Learning Models in the Proposed DBCD-MIT on the Evaluation Criteria

Since this article focuses on a deep learning

method, this section provides a performance comparison between our proposed method and other deep learning approaches. In light of this, we developed three deep models based on the model of basic single input presented in our previous article (8). Table 5 demonstrates the obtained results using the above criteria in this method. As previously mentioned, this study was conducted using fourfold cross-validation.

Therefore, Table 5 shows the evaluation metrics for each fold of every examined network separately. According to Table 5, the average results for the fourfold cross-validation are relatively similar among the three examined networks. Given the importance of the sensitivity parameter in medical applications, the Xception model can be considered well-fitted. This network’s sensitivity is increased by 4% and 6% compared to InceptionV3 and VGG19 architectures, respectively. Based on these findings, the Xception model exhibits a well-suited fit compared to another mode.

Then, it was attempted to improve the results using the proposed DBCD-MIT model. It may be observed in Table 6 that the results obtained by using the proposed method are discussed in detail. DenseNet121 demonstrates a significant advantage over other structures in terms of correctness and concentration, as shown in the results obtained from this model. Consequently, this network has a sensitivity parameter higher

Table 5: Result of three pre-trained networks in the basic single input model

Fold	InceptionV3					Xception					VGG19				
	ACC	Pre	Sn	Sp	F-score	ACC	Pre	Sn	Sp	F-score	ACC	Pre	Sn	Sp	F-score
1	0.73	0.88	0.35	0.97	0.66	0.69	0.70	0.70	0.67	0.70	0.69	1	0.42	1	0.59
2	0.91	0.91	0.93	0.90	0.91	0.85	0.81	0.90	0.80	0.85	0.84	0.86	0.83	0.86	0.84
3	0.92	0.90	0.94	0.91	0.91	0.93	0.93	0.91	0.95	0.91	0.83	0.81	0.88	0.87	0.84
4	0.85	0.80	0.96	0.71	0.87	0.87	0.91	0.81	0.92	0.85	0.91	0.86	0.95	0.88	0.91
Ave	0.85	0.87	0.79	0.87	0.83	0.83	0.84	0.83	0.83	0.82	0.82	0.88	0.77	0.88	0.79

Table 6: Result of three pre-trained networks in the proposed DBCD-MIT model

Fold	VGG16					ResNet50					DeseNet121				
	ACC	Pre	Sn	Sp	F-score	ACC	Pre	Sn	Sp	F-score	ACC	Pre	Sn	Sp	F-score
1	0.98	1	0.97	1	0.98	0.88	0.89	0.91	0.95	0.90	0.95	0.90	1	0.90	0.94
2	0.84	0.88	0.76	0.90	0.81	0.92	0.97	0.91	0.94	0.94	0.98	1	0.96	1	0.97
3	0.90	0.91	0.91	0.88	0.91	0.84	0.67	1	0.76	0.80	0.90	1	0.84	1	0.91
4	0.96	0.9	1	0.94	0.95	0.88	1	0.70	1	0.82	0.90	0.87	0.87	0.91	0.87
Ave	0.92	0.93	0.91	0.93	0.92	0.88	0.88	0.88	0.88	0.87	0.93	0.94	0.92	0.95	0.93

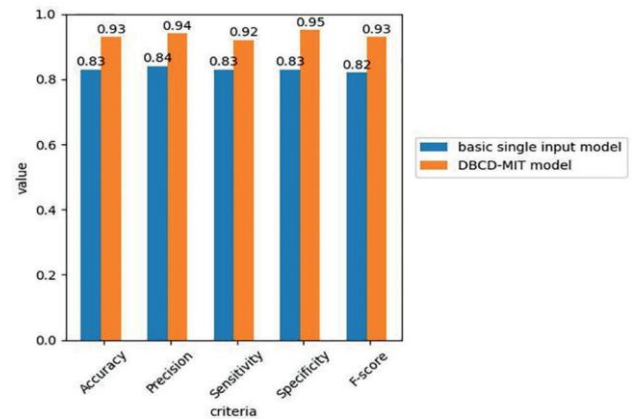
than those of both the VGG16 and ResNet50 networks, resulting in a 1% and 4% increase, respectively, in sensitivity. Additionally, Densenet121 had fourfold improved results compared with VGG16 and ResNet50.

As shown in Figure 10, the average obtained results indicate that the proposed DBCD-MIT model performs significantly better than the basic single input model. As a result of this scenario, it may be observed that using dynamic filters in combination with transfer learning to process each view of the thermograms separately can increase accuracy, precision, sensitivity, specificity, and F-score of 10%, 10%, 9%, 12%, and 11%, respectively, over a transfer learning model for all views of the thermogram.

Comparison between the Proposed Method and other Methods

In the previous section, a limited number of results from the proposed and alternative methods were visually presented in the form of various thermograms demonstrating the improvement brought about by the proposed method in this article. This section presents the numerical results of comprehensive tests on the entire dataset for both the proposed method and its alternatives, highlighting the significant improvements brought by the proposed method in this article.

As previously mentioned, breast cancer detection using thermography can be classified

**Figure 10:** The comparison between the basic single-input model and the proposed DBCD-MIT model

into two categories: deep learning and traditional methods. In this section, the comparison is conducted between the proposed method and either deep learning-based or traditional feature-based methods, which were previously published in this domain. As we used the DMR dataset in this study, the results were compared to those of articles that employed the same dataset. Table 7 compares the proposed DBCD-MIT model and the deep-based methods, demonstrating that the proposed scheme leads to higher values for almost all parameters versus other methods. Compared to its closest alternative, the proposed method has a sensitivity and specificity gain of at least 1% and 2%, respectively.

The introduction of this article mentions various methods for diagnosing cancer based on

Table 7: Comparison of the proposed DBCD-MIT model with deep learning-based methods

Method	ACC	Pre	Sn	Sp	F-score
(4)	0.90	0.93	0.93	0.83	-
(37)	0.92	0.94	0.91	0.93	0.92
(38)	0.80	0.71	0.83	0.77	0.76
(39)	0.77	-	0.85	0.70	0.76
(40)	0.80	0.88	0.86	0.86	0.87
(41)	0.92	-	-	-	-
(42)	0.88	-	-	-	-
(43)	0.90	-	0.87	0.92	-
Ours	0.93	0.94	0.92	0.95	0.93

Table 8: Comparison of the proposed DBCD-MIT model with some handcrafted-based methods

Method	ACC	Sn	Sp
(15)	0.91	0.87	0.94
(16)	0.73	0.78	0.88
(44)	0.88	0.80	0.93
(45)	0.85	0.87	0.83
(46)	0.90	0.87	0.92
Ours	0.93	0.92	0.95

thermographic images that use feature extraction and traditional classifier methods. Due to this, the proposed method was compared with traditional methods that extract features manually, as shown in Table 8. Most of these methods utilize a segmentation technique to extract texture, statistical features, GLCM, Haralick, wavelet, HOG, etc., from thermograms.

Discussion

It has been noted before that manual processing of thermograms is both time-consuming and tedious, as well as requiring expertise from physicians. In recent years, computer-aided detection systems have become a reliable means of interpreting breast thermography images thanks to the development of machine learning algorithms. Obtaining significant results from the breast thermogram mainly involves extracting certain features and analyzing and comparing these features. Traditional techniques include manually extracting features and classifying them using machine learning algorithms. One of the main challenges of this approach is selecting the appropriate feature and Classification (5). Unlike traditional machine learning methods, deep learning can extract high-level features, even with a large amount of training data. To increase the effectiveness of the deep model, it is possible to fuse the related features of thermograms from different patient views. In this study, the primary objective was to develop a system with acceptable accuracy to detect breast cancer when fusing the information available in different views of thermograms.

This study utilizes a dynamic DBCD-MIT method to identify and combine relevant features from five views of breast thermograms. This framework consists of four steps: after extracting each thermogram's valuable features independently, the valuable features are weighted by dynamically generating a filter. A single feature vector can then be utilized as a basis for

Classification by condensing useful features.

Using deep learning, Table 7 compares the proposed and state-of-the-art algorithms. Even though the Sn parameter had a relatively low superiority in the study (4), the value of the Sp parameter differed significantly from that obtained by our method. Using the system presented in the study (4), multiple breast thermogram views are combined with corresponding clinical data for improved diagnosis accuracy. This superiority of 12% in the Sp parameter obtained by our method demonstrates the effectiveness of the proposed mechanism in identifying useful features through the dynamic generation of filters.

The dynamic filtering approach employed in the DBCD-MIT model is central to its success. The system effectively filters out redundancies and emphasizes diagnostically relevant information by dynamically assigning weights to features from different thermogram views. This contrasts sharply with conventional single-view or static multi-view systems, which often fail to account for inter-view dependencies and redundancies, leading to suboptimal performance. It should be noted that the higher specificity obtained (39) results from an unbalanced dataset that has been utilized for training the model. Furthermore, in medical applications, sensitivity is the most important parameter; thus, the superiority of the results of the proposed method, with a 4% improvement in sensitivity against this particular alternative, is also justified.

It is evident from Table 8 that the proposed method is superior to handcrafted feature-based schemes. Due to the lack of reported values in the references, the precision and F-score parameters have been removed from this table. However, compared with other methods, the superiorities of sensitivity and specificity parameters belonging to DBCD-MIT have been calculated in a range of 5-14% and 1-12%, respectively. Traditional handcrafted methods, reliant on feature extraction techniques such as

texture and shape analysis, achieved 78% and 87% sensitivities. In comparison, the DBCD-MIT model consistently surpassed these figures, achieving sensitivities as high as 92% while maintaining high specificity. This demonstrates the limitations of handcrafted approaches in capturing the intricate, high-dimensional relationships inherent in thermographic data.

Among deep learning models, those utilizing transfer learning frameworks such as ResNet50 and DenseNet121 were outperformed by the DBCD-MIT model. Integrating dynamic filters in the proposed method provided a distinct edge, as evidenced by the superior performance metrics across multiple cross-validation folds. The comparative advantage of DBCD-MIT over these models highlights the importance of dynamic, adaptive processing in complex diagnostic tasks.

The advancements achieved by the DBCD-MIT model carry profound implications for clinical practice. The enhanced sensitivity reduces the likelihood of missed cancer cases, a critical concern given the severe consequences of delayed diagnoses. High specificity, on the other hand, mitigates unnecessary anxiety and invasive procedures for patients, contributing to an improved overall patient experience. Moreover, the model's reliance on thermography—a non-invasive, radiation-free, and cost-effective imaging modality—makes it particularly suitable for widespread screening, including in resource-limited settings where access to mammography and histopathology may be constrained.

Conclusion

This article proposed a new method to improve breast cancer diagnosis in multi-input thermographic images. In this method, dependency extraction between thermograms captured from several views in parallel with removing their redundancies was used to improve the distinguishing between healthy and sick samples. Dynamic filters were utilized to enrich the above information, which were constructed separately for each view. In the first and second tests of experiments, it was shown that fusing data in the proposed way improved the detection of breast cancer by up to 9% in sensitivity and up to 12% in specificity compared to a similar deep learning method in which the above processing was not used. In this way, the effectiveness of this data processing method in improving the results

was proven. On the other hand, the comparison of the proposed method with the state-of-the-art methods that have a different approach from our proposed method also indicated the effectiveness of this technique in such a way that it achieved improvements of up to 14% and 25% for sensitivity and specificity compared to the known researches in this field. The above findings indicated that the proposed method is recommended as a part of the processing in different machine learning algorithms that are used to separate healthy and sick data based on multi-input thermograms due to its effective improvement in the quality of input data to the classifier.

Funding

The authors received no financial support for this article's research, authorship, and/or publication.

Conflict of Interest

There are no conflicts of interest.

References

1. Jalloul R, Chethan HK, Alkhatib R. A Review of Machine Learning Techniques for the Classification and Detection of Breast Cancer from Medical Images. *Diagnostics (Basel)*. 2023;13(14). doi: 10.3390/diagnostics13142460.
2. Jakkaladiki SP, Maly F. An efficient transfer learning based cross model classification (TLBCM) technique for the prediction of breast cancer. *PeerJ Comput Sci*. 2023;9:e1281. doi: 10.7717/peerj-cs.1281.
3. Ekici S, Jawzal H. Breast cancer diagnosis using thermography and convolutional neural networks. *Med Hypotheses*. 2020;137:109542. doi: 10.1016/j.mehy.2019.109542.
4. Tsietsos D, Yahya A, Samikannu R, Tariq MU, Babar M, Qureshi B, et al. Multi-input deep learning approach for breast cancer screening using thermal infrared imaging and clinical data. *IEEE Access*. 2023;11:52101-16. doi: 10.1109/ACCESS.2023.3280422.
5. Ensafi M, Keyvanpour MR, Shojaedini SV. ABT: a comparative analytical survey on Analysis of Breast Thermograms. *Multimedia Tools and Applications*. 2024;83(18):53293-346. doi: 10.1007/s11042-023-17566-1.
6. Mashekova A, Zhao Y, Ng EY, Zarikas V, Fok SC, Mukhmetov O. Early detection of the breast cancer using infrared technology—A

- comprehensive review. *Thermal Science and Engineering Progress*. 2022;27:101142. doi: 10.1016/j.tsep.2021.101142.
7. Wen X, Guo X, Wang S, Lu Z, Zhang Y. Breast cancer diagnosis: A systematic review. *Biocybernetics and Biomedical Engineering*. 2024;44(1):119-48. doi: 10.1016/j.bbe.2024.01.002.
 8. Ensafi M, Keyvanpour MR, Shojaedini SV. A New method for promote the performance of deep learning paradigm in diagnosing breast cancer: improving role of fusing multiple views of thermography images. *Health Technol (Berl)*. 2022;12(6):1097-107. doi: 10.1007/s12553-022-00702-6.
 9. Resmini R, Faria da Silva L, Medeiros PRT, Araujo AS, Muchaluat-Saade DC, Conci A. A hybrid methodology for breast screening and cancer diagnosis using thermography. *Comput Biol Med*. 2021;135:104553. doi: 10.1016/j.combiomed.2021.104553.
 10. Nogales A, Perez-Lara F, García-Tejedor AJ. Enhancing breast cancer diagnosis with deep learning and evolutionary algorithms: A comparison of approaches using different thermographic imaging treatments. *Multimedia Tools and Applications*. 2024;83(14):42955-71. doi: 10.1007/s11042-023-17281-x.
 11. Singh D, Singh AK. Role of image thermography in early breast cancer detection- Past, present and future. *Comput Methods Programs Biomed*. 2020;183:105074. doi: 10.1016/j.cmpb.2019.105074.
 12. Tariq M, Iqbal S, Ayesha H, Abbas I, Ahmad KT, Niazi MFK. Medical image based breast cancer diagnosis: State of the art and future directions. *Expert Systems with Applications*. 2021;167:114095. doi: 10.1016/j.eswa.2020.114095.
 13. Bhatt C, Kumar I, Vijayakumar V, Singh KU, Kumar A. The state of the art of deep learning models in medical science and their challenges. *Multimedia Systems*. 2021;27(4):599-613. doi: 10.1007/s00530-020-00694-1.
 14. Nikoupour M, Keyvanpour MR, Shojaedini SV, editors. A robust framework for epileptic seizure diagnosis: Utilizing gru-cnn architectures in eeg signal analysis. 2024 20th CSI International Symposium on Artificial Intelligence and Signal Processing (AISP); 2024. doi: 10.1109/AISP61396.2024.10475276.
 15. Sathish D, Kamath S, Prasad K, Kadavigere R. Role of normalization of breast thermogram images and automatic classification of breast cancer. *The Visual Computer*. 2019;35:57-70. doi: 10.1007/s00371-017-1447-9.
 16. Santana MAd, Pereira JMS, Silva FLd, Lima NMd, Sousa FNd, Arruda GMSd, et al. Breast cancer diagnosis based on mammary thermography and extreme learning machines. *Research on Biomedical Engineering*. 2018;34:45-53. doi: 10.1590/2446-4740.05217.
 17. Dey A, Ali E, Rajan S. Bilateral symmetry-based abnormality detection in breast thermograms using textural features of hot regions. *IEEEOpen Journal of Instrumentation and Measurement*. 2023;2:1-14. doi: 10.1109/OJIM.2023.3302908.
 18. Mishra V, Rath S, Rath, S.K Local and Global Thresholding-Based Breast Cancer Detection Using Thermograms. In: Singh P, editors. *Machine Learning and Computational Intelligence Techniques for Data Engineering*. MISP. Lecture Notes in Electrical Engineering. 2022;998. doi: 10.1007/978-981-99-0047-3_67.
 19. Gonzalez-Leal R, Kurban M, López-Sánchez L, Gonzalez F. Automatic breast cancer detection on breast thermograms. 6–10 July 2020. Porto: 15th Quantitative InfraRed Thermography Conference; 2020. doi: 10.21611/qirt.2020.100.
 20. Razzak MI, Naz S, Zaib A. Deep learning for medical image processing: Overview, challenges and the future. *Classification in BioApps: Automation of decision making*. 2017:323-50. doi: 10.1007/978-3-319-65981-7_12.
 21. Anwar SM, Majid M, Qayyum A, Awais M, Alnowami M, Khan MK. Medical Image Analysis using Convolutional Neural Networks: A Review. *J Med Syst*. 2018;42(11):226. doi: 10.1007/s10916-018-1088-1.
 22. AlFayez F, El-Soud MWA, Gaber T. Thermogram breast cancer detection: A comparative study of two machine learning techniques. *Applied Sciences*. 2020;10(2):551. doi: 10.3390/app10020551.
 23. Tello-Mijares S, Woo F, Flores F. Breast Cancer Identification via Thermography Image Segmentation with a Gradient Vector

- Flow and a Convolutional Neural Network. *J Healthc Eng.* 2019;2019:9807619. doi: 10.1155/2019/9807619.
24. Al Husaini MAS, Habaebi MH, Hameed SA, Islam MR, Gunawan TS. A systematic review of breast cancer detection using thermography and neural networks. *IEEE Access.* 2020;8:208922-37. doi: 10.1109/ACCESS.2020.3038817
 25. Mishra S, Prakash A, Roy SK, Sharan P, Mathur N, editors. Breast cancer detection using thermal images and deep learning. 2020 7th International Conference on Computing for Sustainable Global Development (INDIACom); 2020. p. 211-6. doi: 10.1109/ACCESS.2020.3038817.
 26. Mohamed EA, Rashed EA, Gaber T, Karam O. Deep learning model for fully automated breast cancer detection system from thermograms. *PloS one.* 2022;17(1):e0262349. doi: 10.1371/journal.pone.0262349
 27. Morid MA, Borjali A, Del Fiol G. A scoping review of transfer learning research on medical image analysis using ImageNet. *Computers in biology and medicine.* 2021;128:104115.
 28. Dey S, Roychoudhury R, Malakar S, Sarkar R. Screening of breast cancer from thermogram images by edge detection aided deep transfer learning model. *Multimed Tools Appl.* 2022;81(7):9331-49. doi: 10.1007/s11042-021-11477-9.
 29. Davies S, Jacob J. Novel Algorithms for Early Cancer Diagnosis Using Transfer Learning with MobileNetV2 in Thermal Images. *KSII Transactions on Internet & Information Systems.* 2024;18(3). doi: 10.3837/tiis.2024.03.003.
 30. Alshehri A, AlSaeed D. Breast cancer diagnosis in thermography using pre-trained vgg16 with deep attention mechanisms. *Symmetry.* 2023;15(3):582. doi: 10.3390/sym15030582.
 31. Alshehri A, AlSaeed D. Breast cancer detection in thermography using convolutional neural networks (cnns) with deep attention mechanisms. *Applied Sciences.* 2022;12(24):12922. doi: 10.3390/app122412922.
 32. Tiwari D, Dixit M, Gupta K. Breast cancer-caps: a breast cancer screening system based on capsule network utilizing the multiview breast thermal infrared images. *Turkish Journal of Electrical Engineering and Computer Sciences.* 2022;30(5):1804-20. doi: 10.55730/1300-0632.3906.
 33. Silva L, Saade D, Sequeiros G, Silva A, Paiva A, Bravo RdS, et al. A new database for breast research with infrared image. *Journal of Medical Imaging and Health Informatics.* 2014;4(1):92-100. doi: 10.1166/jmih.2014.1226.
 34. [online]: Available from: <http://visual.ic.uf.br/>
 35. Houssein EH, Emam MM, Ali AA, Suganthan PN. Deep and machine learning techniques for medical imaging-based breast cancer: A comprehensive review. *Expert Systems with Applications.* 2021;167:114161. doi: 10.1016/j.eswa.2020.114161.
 36. Tsietso D, Yahya A, Samikannu R. A review on thermal imaging-based breast cancer detection using deep learning. *Mobile Information Systems.* 2022;2022(1):8952849. doi: 10.1155/2022/8952849.
 37. Zuluaga-Gomez J, Al Masry Z, Benaggonne K, Meraghni S, Zerhouni N. A CNN-based methodology for breast cancer diagnosis using thermal images. *Computer Methods in Biomechanics and Biomedical Engineering: Imaging & Visualization.* 2021;9(2):131-45. doi: 10.1080/21681163.2020.1824685.
 38. Farooq MA, Corcoran P, editors. Infrared imaging for human thermography and breast tumor classification using thermal images. 2020 31st Irish signals and systems conference (ISSC); 2020: IEEE.1-6.
 39. Chaves E, Goncalves CB, Albertini MK, Lee S, Jeon G, Fernandes HC. Evaluation of transfer learning of pre-trained CNNs applied to breast cancer detection on infrared images. *Appl Opt.* 2020;59(17):E23-E8. doi: 10.1364/AO.386037.
 40. Firouzmand M, Majidzadeh K, Jafari M, Haghghat S, Esmaeili R, Moradi L, et al. A Framework for Promoting Passive Breast Cancer Monitoring: Deep Learning as an Interpretation Tool for Breast Thermograms. *Iranian Journal of Medical Physics.* 2024;21(4):237-48. doi: 10.22038/ijmp.2023.71683.2268.
 41. Mammoottil MJ, Kulangara LJ, Cherian AS, Mohandas P, Hasikin K, Mahmud M. Detection of Breast Cancer from Five-View Thermal Images Using Convolutional Neural Networks. *J Healthc Eng.* 2022;2022:4295221. doi: 10.1364/AO.386037.

42. Rautela K, Kumar D, Kumar V, editors. An interpretable network to thermal images for breast cancer detection. 2022 International Conference on Electrical, Computer, Communications and Mechatronics Engineering (ICECCME); 2022. doi: 10.1109/ICECCME55909.2022.9987808.
43. Kiyemet S, Aslankaya MY, Taskiran M, Bolat B, editors. Breast cancer detection from thermography based on deep neural networks. 2019 Innovations in Intelligent Systems and Applications Conference (ASYU); 2019. doi: 10.1109/ASYU48272.2019.8946367.
44. Bohlouli M, Keyvanpour MR, Shojaedini SV, editors. Enhancing Breast Cancer Detection from Thermographic Images: A Hybrid Approach Using Transfer Learning and Generative Adversarial Networks. 2024 10th International Conference on Web Research (ICWR); 2024. p. 27-31. doi: 10.1109/ICWR61162.2024.10533359.
45. Gogoi UR, Bhowmik MK, Ghosh AK, Bhattacharjee D, Majumdar G, editors. Discriminative feature selection for breast abnormality detection and accurate classification of thermograms. 2017 international conference on innovations in electronics, signal processing and communication (IESPC); 2017. p. 39-44. doi: 10.1109/IESPC.2017.8071861.
46. Lessa V, Marengoni M, editors. Applying artificial neural network for the classification of breast cancer using infrared thermographic images. International conference on computer vision and graphics; 2016. p. 429-38. doi: 10.1007/978-3-319-46418-3_38.